LOCAL MESHLESS COLLOCATION SCHEME FOR NUMERICAL SIMULATION OF SPACE FRACTIONAL PDE

by

Mehnaz SHAKEEL[a], Muhammad Nawaz KHAN[b], Imtiaz AHMAD[c], Hijaz AHMAD[d,e], Nantapat JARASTHITIKULCHAI[f*], and Weerawat SUDSUTAD[g]

[a] Shaheed Benazir Bhutto Women University, Peshawar, Pakistan
[b] University of Engineering and Technology, Peshawar, Pakistan
[c] Department of Mathematics, University of Swabi, Khyber Pakhtunkhwa, Pakistan
[d] Operational Research Center in Healthcare, Near East University, Nicosia/Mersin, Turkey
[e] Section of Mathematics, International Telematic University Uninettuno, Roma, Italy
[f] Department of General Education, Faculty of Science and Health Technology, Navamindradhiraj University, Bangkok, Thailand
[g] Department of Statistics, Faculty of Science, Ramkhamhaeng University, Bangkok, Thailand

Original scientific paper
https://doi.org/10.2298/TSCI23S1101S

In this work, numerical solution of multi term space fractional PDE is calculated by using radial basis functions. The fractional derivatives of radial basis functions are evaluated by Caputo and Riemann-Liouville definitions. Local radial basis functions are applied to get stable and accurate solution the problem. Accuracy of the method is assessed by using double mesh procedure. Numerical solutions are presented for different fractional orders to show the effect of introducing fractionality.

Key words: *meshless method, Caputo derivative, space fractional, radial basis functions*

Introduction

The fractional-order models are considered to be more accurate than the integer-order models [1], which is the most important advantage of fractional-order models. This is because fractional PDE take into account the fact that many physical phenomena are non-local, meaning that they cannot be accurately described by methods that only consider local interactions. Space fractional PDE (SFPDE) have the potential to revolutionize the field of mathematics and its applications. They have attracted much attention from researchers in many fields such as physics, engineering, and applied mathematics.

The SFPDE can be used to model a variety of engineering problems. For example, they can be used to model diffusion in porous media, heat transfer in heterogeneous materials, wave propagation in disordered media, anomalous transport, fluid-flow in fractured rocks, hereditary elasticity, and chaotic dynamics [2, 3]. The SFPDE are often used in economics and finance to model certain phenomena. For example, they can be used to model the diffusion of a quantity over time or space. To model the evolution of stock prices over time. These equations

* Corresponding author, e-mail: nantapat.j@nmu.ac.th

allow for the incorporation of features such as jumps and volatility clustering, which are not possible with traditional differential equations.

Since numerical solutions of SFPDE are frequently sufficient, in the absence of exact closed form solutions, numerous numerical techniques have been proposed to solve SFPDE, including finite difference methods [4, 5], general Pade approximation [6], meshless point interpolation method [7], discontinues Galerkin method [8], finite element methods [9, 10], finite volume method [11], RBF Kansa method [12], spline approximation method [13], polynomial and fractional spectral collocation methods [14, 15]. Tadjeran *et al.* [16] also shown how to create numerous high order schemes using the Taylor expansion of the error of the shifted Grünwald method. Zhou *et al.* [17], proposed a third order strategy by combining these assumptions with a compact technique.

Meshless approaches based on RBF have recently been used to solve various forms of FPDEs. To obtain the TFDE solution, in [18] authors used an implicit meshless collocation approach. They also examined the method's convergence and stability both theoretically and numerically. Gu [19] used an implicit meshless methodology based on RBF to solve numerically the anomalous subdiffusion equation and demonstrated the method's convergence and stability. Liu [20] used an implicit meshless approach based on RBF to solve TFDE. Zhuang *et al.* [21] solved the fractional advection-diffusion equation using an implicit meshless approach based on the MLS approximation. In [22], the 1- and 2-D time fractional non-linear Schrodinger equations were solved numerically based on RBF. Liu *et al*. [23] used FDM to discretize the time variable and a meshless approach based on RBF to discretize the space variable to determine the solution of the time fractional mobile/immobile transport model. The authors also investigated the method's convergence and stability.

Fractional derivative of RBF

The fractional derivative (FD) of RBF can be approximated:

$$\mathfrak{D}^{\eta}\,\bar{\mathfrak{u}}(r) = \mathfrak{D}^{\eta}\,\bar{\mathfrak{u}}(|\,\mathfrak{x}-\mathfrak{y}\,|), \quad \text{for all } \mathfrak{x},\mathfrak{y}\in\mathbb{R}$$

where $\mathfrak{D}^{\eta}$ is the FD and $\bar{\mathfrak{u}}(r)$ is the RBF. The following theorems illustrate that finding the FD of $\bar{\mathfrak{u}}$ can result in RBF in one dimension.

Fractional derivative of MQ

Consider the following generalised MQ-RBF:

$$\bar{\mathfrak{u}}(\mathfrak{d}) = \left(1+\mathfrak{d}^2/2\right)^{\gamma/2},\ \gamma\in\mathbb{R} \tag{1}$$

where $\mathfrak{d} = cr$, r is the Euclidian distance, and c is the shape parameter.

Theorem 1. For $\bar{\mathfrak{u}}(\mathfrak{d})$ given in eq. (1), the following results hold for $\mathfrak{d} > 0$:

$${}^{RL}\mathfrak{D}_{\mathfrak{d}}^{\eta}\left(1+\frac{\mathfrak{d}^2}{2}\right)^{\gamma} = \frac{\mathfrak{d}^{\eta}}{\Gamma(1-\eta)}F_{22}\left(\frac{1}{2},1,-\frac{\gamma}{2};\frac{1-\eta}{2},\frac{2-\eta}{2};-\frac{\mathfrak{d}^2}{2}\right)$$

$${}^{C}\mathfrak{D}_{\mathfrak{d}}^{\eta}\left(1+\frac{\mathfrak{d}^2}{2}\right)^{\gamma/2} = \frac{\mathfrak{d}^{\eta}}{\Gamma(1-\eta)}F_{32}\left(\frac{1}{2},1,-\frac{\gamma}{2};\frac{1-\eta}{2},\frac{2-\eta}{2};-\frac{\mathfrak{d}^2}{2}\right)$$

where ${}^{RL}\mathfrak{D}_{\mathfrak{d}}^{\eta}$ is the Riemann-Liouville FD and ${}^{C}\mathfrak{D}_{\mathfrak{d}}^{\eta}$ – the Caputo FD.

Proof: The Taylor series expansion of $\bar{u}(\mathfrak{d})$ about the center $\mathfrak{d} = 0$:

$$\left(1+\frac{\mathfrak{d}^2}{2}\right)^{\gamma/2} = \sum_{n=0}^{\infty} \frac{\left(\frac{\gamma}{2}\right)^{(n)}}{2^n n!} \mathfrak{d}^{2n}$$

therefore

$$\begin{aligned}
{}^{RL}\mathfrak{D}_{\mathfrak{d}}^{\eta}\left(1+\frac{\mathfrak{d}^2}{2}\right)^{\gamma/2} &= {}^{2n}\sum_{n=0}^{\infty} \frac{(-1)^n\left(-\frac{\gamma}{2}\right)_n}{2^n n!}\, {}_0\mathfrak{D}_d^{\eta}\mathfrak{d} \\
&= \sum_{n=0}^{\infty} \frac{(-1)^n\left(-\frac{\gamma}{2}\right)_n}{2^n n!} \frac{\Gamma(2n+1)}{\Gamma(2n-\eta+1)} \mathfrak{d}^{2n-\eta} \\
&= \frac{\mathfrak{d}^{-\eta}}{\Gamma(1-\eta)} \sum_{n=0}^{\infty} \frac{(1)_{2n}\left(-\frac{\gamma}{2}\right)_n}{(1-\eta)_{2n} n!} \left(-\frac{\mathfrak{d}^2}{2}\right)^n \\
&= \frac{\mathfrak{d}^{-\eta}}{\Gamma(1-\eta)} \sum_{n=0}^{\infty} \frac{(1)_n\left(\frac{1}{2}\right)_n\left(-\frac{\gamma}{2}\right)_n}{\left(\frac{2-\eta}{2}\right)_n\left(\frac{1-\eta}{2}\right)_n n!} \left(-\frac{\mathfrak{d}^2}{2}\right)^n \\
&= \frac{\mathfrak{d}^{-\eta}}{\Gamma(1-\eta)} F_{32}\left(\frac{1}{2},1,-\frac{\gamma}{2};\frac{1-\eta}{2},\frac{2-\eta}{2};-\frac{\mathfrak{d}^2}{2}\right)
\end{aligned}$$

also

$${}^{C}\mathfrak{D}_{\mathfrak{d}}^{\eta}\left(1+\frac{\mathfrak{d}^2}{2}\right)^{\gamma/2} = \sum_{n=0}^{\infty} \frac{(-1)^n\left(-\frac{\gamma}{2}\right)_n}{2^n n!}\, {}^{C}{}_{0}\mathfrak{D}_d^{\eta}\mathfrak{d}^{2n} = \frac{\mathfrak{d}^{-\eta}}{\Gamma(1-\eta)} F_{32}\left(\frac{1}{2},1,-\frac{\gamma}{2};\frac{1-\eta}{2},\frac{2-\eta}{2};-\frac{\mathfrak{d}^2}{2}\right)$$

where F_{32} is the generalised hypergeometric function, and $(\mathfrak{d})_{\eta}$ – the Pochhammer symbol, which is defined:

$$(\mathfrak{d})_n = \frac{\Gamma(\mathfrak{d}+n)}{\Gamma(\mathfrak{d})} = \mathfrak{d}(\mathfrak{d}+1)(\mathfrak{d}+2)\cdots(\mathfrak{d}+n-1)$$

$$(\mathfrak{d})_{2n} = 2^{2n}\left(\frac{\mathfrak{d}}{2}\right)_n\left(\frac{1+\mathfrak{d}}{2}\right)_n$$

Fractional derivative of GA

Consider the GA-RBF:

$$\bar{u}(\mathfrak{x}) = \exp\left(\frac{-\mathfrak{x}^2}{2}\right) \tag{2}$$

Theorem 2. For $\bar{u}(\mathfrak{x})$ given in eq. (2), the following results hold for $\mathfrak{x} > 0$:

$$ {}^{RL}\mathfrak{D}_{\mathfrak{x}}^{\eta} e^{-\frac{\mathfrak{x}^2}{2}} = \frac{\mathfrak{x}^{-\eta}}{\Gamma(1-\eta)} F_{22}\left(\frac{1}{2},1;\frac{1-\eta}{2},\frac{2-\eta}{2};-\frac{\mathfrak{x}^2}{2}\right) $$

$$ {}^{C}\mathfrak{D}_{\mathfrak{x}}^{\eta} e^{-\frac{\mathfrak{x}^2}{2}} = \frac{\mathfrak{x}^{-\eta}}{\Gamma(1-\eta)} F_{22}\left(\frac{1}{2},1;\frac{1-\eta}{2},\frac{2-\eta}{2};-\frac{\mathfrak{x}^2}{2}\right) $$

Proof: The Taylor series expansion around the center $\mathfrak{x} = 0$ of $\bar{u}(\mathfrak{x})$:

$$ \mathrm{e}^{-\frac{\mathfrak{x}^2}{2}} = \sum_{n=0}^{\infty} \frac{(-1)^n}{2^n n!} \mathfrak{x}^{2n} $$

therefore

$$ {}^{RL}\mathfrak{D}_{\mathfrak{x}}^{\eta} \mathrm{e}^{-\frac{\mathfrak{x}^2}{2}} = \sum_{n=0}^{\infty} \frac{(-1)^n}{2^n n!} {}_0\mathfrak{D}_{\mathfrak{x}}^{\eta} \mathfrak{x}^{2n} $$

$$ = \sum_{n=0}^{\infty} \frac{(-1)^n}{2^n n!} \frac{\Gamma(2n+1)}{\Gamma(2n-\eta+1)} \mathfrak{x}^{2n-\eta} $$

$$ = \frac{\mathfrak{x}^{-\eta}}{\Gamma(1-\eta)} \sum_{n=0}^{\infty} \frac{(1)_{2n}}{(1-\eta)_{2n} n!} \left(-\frac{\mathfrak{x}^2}{2}\right)^n $$

$$ = \frac{\mathfrak{x}^{-\eta}}{\Gamma(1-\eta)} \sum_{n=0}^{\infty} \frac{(1)_n \left(\frac{1}{2}\right)_n}{\left(\left(\frac{2-\eta}{2}\right)_n \frac{1-\eta}{2}\right)_n n!} \left(-\frac{\mathfrak{x}^2}{2}\right)^n $$

$$ = \frac{\mathfrak{x}^{-\eta}}{\Gamma(1-\eta)} F_{22}\left(\frac{1}{2},1;\frac{1-\eta}{2},\frac{2-\eta}{2};-\frac{\mathfrak{x}^2}{2}\right) $$

Formulation of the scheme

The RBF technique is used in this section derive the numerical solution SFPDE and to determine the FD of unknown function $\bar{u}(\mathfrak{x}, r)$, FD of RBF are used.

The RBF collocation scheme

The function values at a group of collocation points in the region of $\mathfrak{x}_i$ where $i = 1, 2,..., N^n$, are used to interpolate the spatial derivatives of $\bar{u}(\mathfrak{x}, r)$ at the centres $\mathfrak{x}_i$. The RBF estimation of $\bar{u}$:

$$ \bar{u}^m(\mathfrak{x}_k) \approx \sum_{i=1}^{n_k} \lambda_i^m \bar{u}(\mathfrak{x}_k), \ k = 1,2,3,\cdots,M \tag{3} $$

By replacing the RBF function $\bar{u}(\|\mathfrak{x} - \mathfrak{x}_j\|)$ in eq. (3), the coefficients λ_i^m may be calculated:

$$ \bar{u}^{(m)}(\| \mathfrak{x}_i - \mathfrak{x}_l \|) = \sum_{k=1}^{n_i} \lambda_{ik}^{(m)} \bar{u}(\| \mathfrak{x}_k - \mathfrak{x}_l \|), \ l = i_1, \ i_2, \ldots, i_{n_i} \tag{4} $$

In matrix form, eq. (4) is written:

$$\begin{bmatrix} \bar{u}_{i_1}^{(m)}(\mathfrak{x}_i) \\ \bar{u}_{i_2}^{(m)}(\mathfrak{x}_i) \\ \vdots \\ \bar{u}_{i_{n_i}}^{(m)}(\mathfrak{x}_i) \end{bmatrix} = \begin{bmatrix} \bar{u}_{i_1}(\mathfrak{x}_{i_1}) & \bar{u}_{i_2}(\mathfrak{x}_{i_1}) & \cdots & \bar{u}_{i_{n_i}}(\mathfrak{x}_{i_1}) \\ \bar{u}_{i_1}(\mathfrak{x}_{i_2}) & \bar{u}_{i_2}(\mathfrak{x}_{i_2}) & \cdots & \bar{u}_{i_{n_i}}(\mathfrak{x}_{i_2}) \\ \vdots & \vdots & \ddots & \vdots \\ \bar{u}_{i_1}(\mathfrak{x}_{in_i}) & \bar{u}_{i_2}(\mathfrak{x}_{in_i}) & \cdots & \bar{u}_{i_{n_i}}(z_{1_{in_i}}) \end{bmatrix} \begin{bmatrix} \lambda_{i_1}^{(m)} \\ \lambda_{i_2}^{(m)} \\ \vdots \\ \lambda_{i_{n_i}}^{(m)} \end{bmatrix} \tag{5}$$

where

$$\bar{u}_l(\mathfrak{x}_k) = \bar{u}(\| \mathfrak{x}_k - \mathfrak{x}_l \|), \quad l = i_1, i_2, \ldots, i_{n_i}$$

for each $k = i_1, i_2, \ldots, i_{n_i}$.

The matrix form of eq. (5):

$$\bar{u}_{n_i}^{(m)} = A_{n_i} \boldsymbol{\lambda}_{n_i}^{(m)} \tag{6}$$

where

$$\bar{u}_{n_i}^{(m)} = \begin{bmatrix} \bar{u}_{i_1}^{(m)}(\mathfrak{x}_i) & \bar{u}_{i_2}^{(m)}(\mathfrak{x}_i) & \ldots & \bar{u}_{i_{n_i}}^{(m)}(\mathfrak{x}_i) \end{bmatrix}^T$$

$$A_{n_i} = \begin{bmatrix} \bar{u}_{i_1}(\mathfrak{x}_{i_1}) & \bar{u}_{i_2}(\mathfrak{x}_{i_1}) & \cdots & \bar{u}_{i_{n_i}}(\mathfrak{x}_{i_1}) \\ \bar{u}_{i_1}(\mathfrak{x}_{i_2}) & \bar{u}_{i_2}(\mathfrak{x}_{i_2}) & \cdots & \bar{u}_{i_{n_i}}(\mathfrak{x}_{i_2}) \\ \vdots & \vdots & \ddots & \vdots \\ \bar{u}_{i_1}(\mathfrak{x}_{i_{n_i}}) & \bar{u}_{i_2}(\mathfrak{x}_{i_{n_i}}) & \cdots & \bar{u}_{i_{n_i}}(\mathfrak{x}_{i_{n_i}}) \end{bmatrix}$$

$$\boldsymbol{\lambda}_{n_i}^{(m)} = \begin{bmatrix} \lambda_{i_1}^{(m)} & \lambda_{i_2}^{(m)} & \ldots & \lambda_{i_{n_i}}^{(m)} \end{bmatrix}^T$$

From eq. (6), obtain:

$$\boldsymbol{\lambda}_{n_i}^{(m)} = A_{n_i}^{-1} \bar{u}_{n_i}^{(m)} \tag{7}$$

From eqs. (3) and (7):

$$\bar{u}^{(m)}(\mathfrak{x}_i) = A_{n_i}^{-1} \bar{u}_{n_i}^{(m)}(\mathfrak{x}) \bar{u}_{n_i} = V(\mathfrak{x}_i) \bar{u}_{n_i} \tag{8}$$

where

$$\bar{u}_{n_i} = \begin{bmatrix} \bar{u}(\mathfrak{x}_{i_1}), \bar{u}(\mathfrak{x}_{i_2}), \ldots, \bar{u}(\mathfrak{x}_{i_{n_i}}) \end{bmatrix}^T$$

and

$$V(\mathfrak{x}_i) = A_{n_i}^{-1} \bar{u}_{n_i}^{(m)}(\mathfrak{x})$$

Meshless scheme for the solution of SFPDE

The strategy obtained in section *The RBF Collocation scheme* is applied to the SFPDE presented as [24]:

$$\frac{\partial \bar{u}}{\partial \tau} = H(\bar{u}, \mathfrak{D}_{\mathfrak{x}}^{\eta} \bar{u}), \quad \tau \in [0,T], \mathfrak{x} \in \Omega \cup \partial\Omega \tag{9}$$

The initial and boundary conditions:

$$\begin{gathered} \bar{u}(\mathfrak{x},0) = \bar{u}_0, \quad \mathfrak{x} \in \Omega \cup \partial\Omega \\ \bar{u}(\mathfrak{x},\tau) = G(\tau) \quad \tau \in [0,T], \quad \mathfrak{x} \in \partial\Omega \end{gathered} \tag{10}$$

Substituting eq. (8) in eq. (9), we have:

$$\frac{\mathrm{d}\bar{u}_{n_i}}{\mathrm{d}\tau} = H(\mathbf{V}(\mathfrak{x}_i).\bar{u}, \mathfrak{D}_{\mathfrak{x}}^{\eta} \mathbf{V}(\mathfrak{x}_i).\bar{u}) \tag{11}$$

Equation (11) is an ODE system that may be solved using any fast and accurate ODE solver to obtain the solution eq. (9).

Results and discussions

This section aims to evaluate the scheme's performance by applying it to various test problems. The numerical solutions to Test *Problems 1 and 2* are also provided in [25], where the unknown answer is stated using the Lagrange basis, which is defined:

$$L(\mathfrak{x}) = \bar{u}(\mathfrak{x}) A^{-1}$$

which increases the computing cost of the technique. Local RBF are utilised to overcome this limitation.

Test Problem 1. The following initial boundary value problem is considered in the first test problem [24]:

$$\frac{\partial \bar{u}}{\partial \tau} = -K_{\eta} \mathfrak{D}_{\mathfrak{x}}^{\eta} \bar{u}(\mathfrak{x},\tau) \quad \mathfrak{x} \in [0,\pi], \ \tau \in [0,T], \ 1 \le \eta \le 2$$

$$\begin{gathered} \bar{u}(\mathfrak{x},0) = \mathfrak{x}^2 (\pi - \mathfrak{x}) \\ \bar{u}(0,\tau) = \bar{u}(\pi,\tau) = 0 \end{gathered}$$

The values of K_{η}, c, N, T, and $\mathrm{d}\tau$ are 1.25, 100, 101, 1, and 0.001.

The well-known double mesh methodology is used for the convergence of the method due to the lack of an exact solution, and the results are reported in tab. 1. The numerical findings are displayed in figs. 1 and 2, for various values of T and η. The solution's amplitude and steepness increases as the FD order increases, but the solution's amplitude and steepness decrease as time passes. The approach also yields a smooth solution for any value of T.

Table 1. Maximum error for numerous values of η and N for Test *Problem 1*

	N			
η	20	40	80	160
1.8	$2.2685 \cdot 10^{-4}$	$6.0661 \cdot 10^{-5}$	$1.7037 \cdot 10^{-5}$	$4.8619 \cdot 10^{-6}$
1.6	$6.5001 \cdot 10^{-4}$	$1.0986 \cdot 10^{-4}$	$6.8699 \cdot 10^{-5}$	$2.2608 \cdot 10^{-5}$
1.4	$1.3776 \cdot 10^{-3}$	$5.2111 \cdot 10^{-4}$	$1.9713 \cdot 10^{-4}$	$7.4648 \cdot 10^{-5}$
1.2	$2.4919 \cdot 10^{-3}$	$1.0940 \cdot 10^{-3}$	$4.7701 \cdot 10^{-4}$	$2.0770 \cdot 10^{-4}$

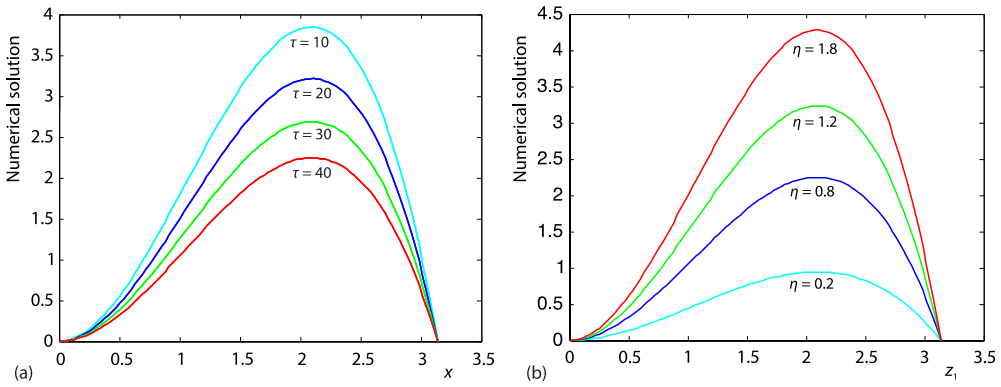

Figure 1. Numerical results for numerous values of time level (a) and η (b) for Test *Problem 1*

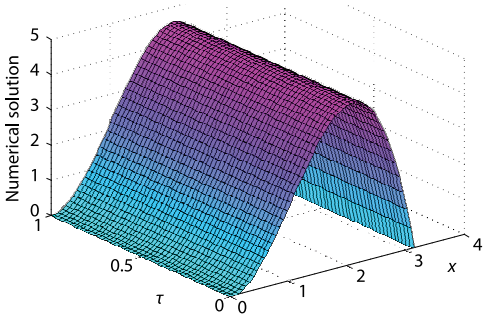

Figure 2. Numerical result using $K_\eta = 0.25$ and $\eta = 1.8$ for Test *Problem 1*

Test Problem 2. The following space fractional advection-dispersion equation (SFADE) is used in the last problem [24]:

$$\frac{\partial \bar{u}}{\partial \tau} = -K_\eta \mathfrak{D}_{\mathfrak{x}}^{\eta} \bar{u}(\mathfrak{x},\tau) - K_{\hat{n}} \mathfrak{D}_{\mathfrak{x}}^{\varrho} \bar{u}(\mathfrak{x},\tau), \quad \mathfrak{x} \in [0,\pi], \quad \tau \in [0,T], \; 1 < \eta \le 2, \; 0 < \varrho \le 1$$

the initial and boundary conditions

$$\bar{u}(\mathfrak{x},0) = \mathfrak{x}^2(\pi - \mathfrak{x}), \quad \bar{u}(0,\tau) = \bar{u}(\pi,\tau) = 0$$

where N, ϱ, η, c, T, and dτ have values of 101, 0.5, 1.2,, 100, 1, and 0.001, respectively. The maximum error for numerous values of N and η are presented in tab. 2 to examine the method's convergence. To determine the values of the E_∞ the double mesh approach is used. In figs. 3 and 4, numerical solutions for various η and ϱ values are presented. The amplitude of the numerical result rises as the value of η increases, as shown in fig. 3, and the amplitude increases when the value of ϱ increases, as shown in fig. 4. Also the numerical solution is visualized in fig. 5 for various parameters values.

Table 2. Maximum error for numerous values of η and N for Test *Problem 2*

	N			
η	16	32	64	128
1.8	$1.5000 \cdot 10^{-05}$	$3.6762 \cdot 10^{-06}$	$9.6471 \cdot 10^{-07}$	$2.5858 \cdot 10^{-07}$
1.6	$9.8924 \cdot 10^{-05}$	$3.2123 \cdot 10^{-05}$	$1.0544 \cdot 10^{-05}$	$3.4762 \cdot 10^{-06}$
1.4	$2.2124 \cdot 10^{-04}$	$8.3640 \cdot 10^{-05}$	$3.1658 \cdot 10^{-05}$	$1.2002 \cdot 10^{-05}$
1.2	$1.0796 \cdot 10^{-02}$	$7.0431 \cdot 10^{-03}$	$4.7057 \cdot 10^{-03}$	$3.2038 \cdot 10^{-03}$

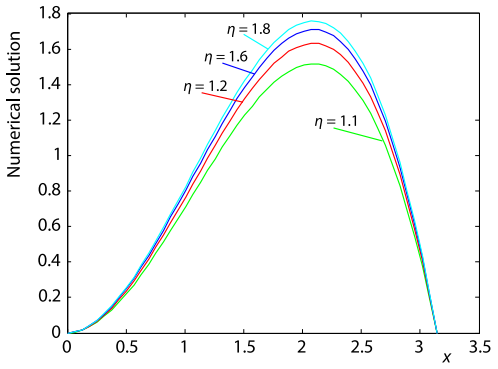

Figure 3. Numerical results for numerous values of η using $N = 51$, $t = 10$, $\varrho = 0.4$ for Test *Problem 2*

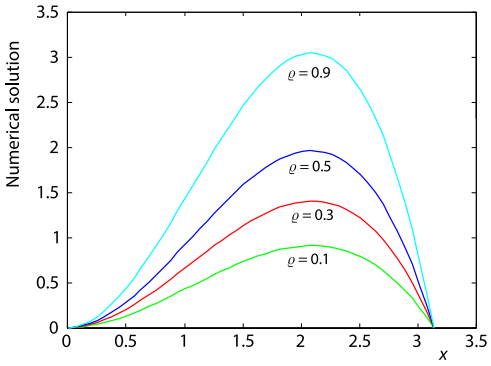

Figure 4. Numerical results for numerous values of ϱ using $N = 51$, $t = 10$, and $\eta = 1.5$ for Test *Problem 2*

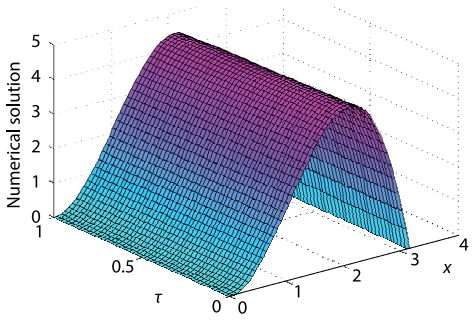

Figure 5. Numerical result using $K_\eta = 0.25$, $\eta = 1.2$, and $\varrho = 0.5$ for Test *Problem 2*

Conclusion

The multi term SFPDE are solved by using local RBF. The fractional derivatives of RBF are represented in terms of hypergeometric function, rather than series form, which reduces the truncation error. Results are compared with some other methods in literature. Results are shown to be accurate with the help of double mesh technique. The advantage of using local RBF is also discussed by comparison with the methods in literature. The results are plotted for different fractional orders which shows the amplitude of the solution depends on the fractional derivative order.

References

[1] Podlubny, I., *Fractional Differential Equations*, Academic Press, New York, USA, 1999
[2] Metzler, R., Klafter, J., The Random Walk's Guide to Anomalous Diffusion: A Fractional Dynamics Approach, *Phys. Rep.*, *339* (2000), 1, pp. 1-77
[3] Zaslavsky, G. M., Chaos, Fractional Kinetics, and Anomalous Transport, *Phys. Rep.*, *371* (2002), 6, pp. 461-580
[4] Meerschaert, M. M., Tadjeran, C., Finite Difference Approximations for Two-Sided Space-Fractional Partial Differential Equations, *Appl. Numer. Math.*, *56* (2006), 1, pp. 80-90
[5] Tian, W. Y., *et al.*, A Class of Second Order Difference Approximations for Solving Space Fractional Diffusion Equations, *Math. Comput.*, *84* (2015), 294, pp. 1703-1727
[6] Ding, H. F., General Pade Approximation Method for Time-Space Fractional Diffusion Equation, *Journal Comput. Appl. Math.*, *299* (2016), C, pp. 221-228
[7] Liu, Q., *et al.*, A Meshless Method Based on Point Interpolation Method (PIM) for the Space Fractional Diffusion Equation, *Appl. Math. Comput.*, *256* (2015), Apr., pp. 930-938

[8] Xu, Q. W., Hesthaven, J. S., Discontinuous Galerkin Method for Fractional Convection-Diffusion Equations, *SIAM J. Numer. Anal*., *52* (2014), 1, pp. 405-423
[9] Ervin, V. J., Roop, J. P., Variational Formulation for the Stationary Fractional Advection Dispersion Equation, *Numer. Methods Partial Differ. Equ*., *22* (2006), 3, pp. 558-576
[10] Zhang, H., *et al*., Galerkin Finite Element Approximation of Symmetric Space-Fractional Partial Differential Equations, *Appl. Math. Comput.*, *217* (2010), 6, pp. 2534-2545
[11] Hejazi, H., Stability and Convergence of a Finite Volume Method for the Space Fractional Advection-Dispersion Equation, *Journal Comput. Appl. Math*., *255* (2014), Jan., pp. 684-697
[12] Pang, G. F., *et al*., Space-Fractional Advection-Dispersion Equations by the Kansa Method, *Journal Comput. Phys.*, *293* (2015), July, pp. 280-296.
[13] Sousa, E., Numerical Approximations for Fractional Diffusion Equations Via Splines, *Comput. Math*. *Appl*., *62* (2011), 3, pp. 938-944
[14] Tian, W. Y., *et al.*, Polynomial Spectral Collocation Method for Space Fractional Advection-Diffusion Equation, *Numer. Methods Partial Differ. Equ*., *30* (2014), 2, pp. 280-296
[15] Zayernouri, M., Karniadakis, G. E., Fractional Spectral Collocation Methods for Linear and Non-Linear Variable Order FPDE, *Journal Comput. Phys*., *293* (2015), July, pp. 312-338
[16] Tadjeran, C., *et al*., A Second-Order Accurate Numerical Approximation for the Fractional Diffusion Equation, *Journal Comput. Phys.*, *213* (2006), 1, pp. 205-213
[17] Zhou, H., *et al*., Quasi-Compact Finite Difference Schemes for Space Fractional Diffusion Equations, *Journal Sci. Comput*., *56* (2013), Nov., pp. 45-66
[18] Gu, Y., *et al*., An Advanced Meshless Method for Time Fractional Diffusion Equation, *Int. J. Comput*. *Methods*, *8* (2011), 4, pp. 653-665
[19] Gu, Y. T., An Advanced Implicit Meshless Approach for the Non-Linear Anomalous Subdiffusion Equation, *Comput. Model. Eng. Sci*., *56* (2010), 3, pp. 303-333
[20] Liu, Q., An Implicit RBF Meshless Approach for Time Fractional Diffusion Equations, *Comput. Mech. 48* (2011), Feb., pp. 1-12
[21] Zhuang, P., *et al.*, Time-Dependent Fractional Advection-Diffusion Equations by an Implicit MLS Meshless Method, I*nt. J. Numer. Methods Engg*., *88* (2011), 13, pp. 1346-1362
[22] Mohebbi, A., *et al*., The Use of a Meshless Technique Based on Collocation and Radial Basis Functions for Solving the Time Fractional Non-Linear Schrodinger equation Arising in Quantum Mechanics, *Engg. Anal. Bound. Elem*., *37* (2013), 2, pp. 475-485
[23] Liu, Q., *et al*., A RBF Meshless Approach for Modelling a Fractal Mobile/Immobile Transport Model, *Appl. Math. Comput*., *226* (2014), Jan., pp. 336-347
[24] Yang, Q., *et al*., Numerical Methods for Fractional Partial Differential Equations with Riesz Space Fractional Derivatives, *Appl. Math. Model*., *34* (2010), 1, pp. 200-218
[25] Maryam, M., Schaback, R., On the Fractional Derivatives of Radial Basis Functions, On-line first, https://arxiv.org/abs/1612.07563, 2016

Paper submitted: February 1, 2022
Paper revised: March 4, 2022
Paper accepted: March 14, 2022